Momentum Flux by Thermally Induced Internal Gravity Waves and Its Approximation for Large-Scale Models

HYE-YEONG CHUN

Department of Atmospheric Sciences and Global Environmental Laboratory, Yonsei University, Seoul, Korea

JONG-JIN BAIK

Department of Environmental Science and Engineering, Kwangju Institute of Science and Technology, Kwangju, Korea

(Manuscript received 9 April 1997, in final form 10 February 1998)

ABSTRACT

Gravity wave momentum flux induced by thermal forcing representing latent heating due to cumulus convection is investigated analytically from a viewpoint of a subgrid-scale drag for the large-scale flow, and a possible way to parameterize the momentum flux in large-scale models is proposed. For the formulations of the momentum flux and its vertical derivative, two-dimensional, steady-state, linear perturbations induced by thermal forcing in a uniform basic-state wind are considered. The calculated momentum flux is zero below the forcing bottom, varies with height in the forcing region, and remains constant above the forcing top with the forcing top value. The sign of the momentum flux at the forcing top depends on the basic-state wind according to the wave energy–momentum flux relationship. Inside the forcing region, there exists a vertical convergence or divergence of the momentum flux that can influence the zonal mean flow tendency. The maximum magnitude of the zonal mean flow tendency contributed by the wave momentum flux in the forcing region is as large as 24 m s^{-1} d^{-1}.

A parameterization scheme of subgrid-scale convection-induced gravity wave momentum flux for use in large-scale models is proposed. Even though the momentum flux in the cloud region can be parameterized based on the analytical formulation, it is not practically applied in large-scale models because subgrid-scale diabatic forcing considered in this study comes from cumulus parameterization that is activated only in a conditionally unstable atmosphere. Thus, the convection-induced momentum flux is parameterized from the cloud-top height. The momentum flux at the cloud-top height is parameterized based on the analytical formulation, while above it two methods can be used following mountain drag parameterization. One method is to specify a linearly decreasing vertical profile with height and the other is to apply the wave saturation theory in terms of the Richardson number criterion. The formulations of the minimum Richardson number and saturation momentum flux are surprisingly analogous to those in mountain drag parameterization except that the nonlinearity factor of thermally induced waves is used instead of the Froude number. Gravity wave drag by convection can have a relatively strong impact on the large-scale flow in midlatitude summertime when the surface wind and stability are weak and in the tropical area where deep cumulus convection persistently exists.

1. Introduction

During the past decade, gravity wave drag has received much attention because it is recognized to be an important subgrid-scale dynamic process in order for the large-scale mean flow to maintain its observed state in general circulation models (GCMs). A missing gravity wave drag was found to cause an underestimation of the vertically integrated total surface stress compared with the horizontal convergence of the poleward momentum flux (Swinbank 1985). It has been shown that the westerly bias of the Northern Hemisphere winter mean flow can be reduced significantly by including orographic gravity wave drag parameterization (e.g., Palmer et al. 1986; McFarlane 1987). Currently, there are two types of theoretical basis for parameterizing orographic gravity wave drag. One is based on the linear saturation theory (Lindzen 1981) indicating possible wave breaking heights in the upper atmosphere and the other on the nonlinear mountain wave theory (Pierrehumbert 1986) indicating wave breaking heights wherever the Froude number is larger than a certain critical value.

Even though the source of gravity wave drag considered thus far in large-scale numerical models comes exclusively from mountains, there is a considerable uncertainty of the dominant tropospheric sources of gravity waves. In a review paper on gravity waves in the middle atmosphere, Fritts (1984) showed that a large portion of observed gravity wave mo-

Corresponding author address: Professor Hye-Yeong Chun, Department of Atmospheric Sciences, Yonsei University, Shinchon-dong, Seadaemun-ku, Seoul 120-749, Korea.
E-mail: chy@atmos.yonsei.ac.kr

mentum flux has higher frequencies than those of stationary mountain waves. One of the alternative sources of gravity waves in the troposphere comes from cumulus convection. In summertime when the surface wind and stability are weak, the magnitude of surface drag and the resultant influence of orographically induced gravity wave drag on the large-scale flow are relatively small compared with those in wintertime (Palmer et al. 1986). In this situation, the relative importance of cumulus convection as a source of gravity waves can be increased. In addition, in the tropical region where persistent convection exists, deep cumulus clouds impinging on the stable stratosphere can generate gravity waves that influence the large-scale flow through gravity wave drag.

Theoretical aspects of thermally induced gravity waves have received less attention than those of mountain-induced gravity waves. Perhaps this might be one of the reasons that gravity wave drag induced by a thermal source and its influence on the large-scale flow have not yet been considered in a systematic way. Besides, most theoretical studies for the response of a stably stratified airflow to thermal forcing have been confined to examining some dynamical aspects of tropospheric phenomena related to thermally induced mesoscale circulation. Using a two-dimensional cloud model, Fovell et al. (1992) investigated convectively generated stratospheric gravity waves under three different mean flow structures in the stratosphere. They concluded that the mechanical effect of convection by oscillating updrafts and downdrafts impinging on the stable interface rather than the thermal effect proposed by Clark et al. (1986) is a dominant mechanism for generating gravity waves by convection. The momentum flux induced by simulated squall lines in the lower stratosphere is about -0.2 N m^{-2}, which produces an associated zonal mean flow tendency of -20 m s^{-1} d^{-1} (Fovell et al. 1992). This is even larger than the gravity wave drag induced by midlatitude orography. Recently, Kershaw (1995) formulated momentum flux by convectively generated internal gravity waves in constant basic-state wind and stability under the assumption that wave energy above the convective region is proportional to the convective kinetic energy in the cloud region. For the case of small Froude number, the momentum flux is shown to be proportional to the basic-state wind relative to the moving convection and convective intensity in terms of maximum vertical velocity in the convective region and inversely proportional to the Brunt–Väisälä frequency. Through the simulations of precipitating convective clouds, parameterization of momentum flux was validated and the proportionality constant in converting convection to wave energy was estimated.

Significance of the thermally induced momentum flux compared with the mountain-induced momentum flux was pointed out by Smith and Lin (1982). From the linear, steady-state response of a stably stratified airflow to diabatic heating representing latent heating associated with orographic rain, they showed that the magnitude of the momentum flux by thermal forcing with constant heating rate estimated from a typical precipitation rate can be even larger than that by a mountain with a height of 500 m under the same mean wind and stability. Besides, there exists a vertical convergence/divergence of the momentum flux wherever thermal forcing is located (Lin 1987; Chun and Baik 1994). Recently, Chun (1997) examined the weakly nonlinear response of a stably stratified shear flow to diabatic forcing and showed that there exists a nonzero vertical convergence/divergence of the momentum flux even above the thermal forcing region for the weakly nonlinear perturbations. The vertical convergence/divergence of the momentum flux is also nonzero above the thermal forcing in the transient, linear response of a stably stratifed shear flow to thermal forcing (Baik et al. 1998).

Existence of a vertical convergence/divergence of the momentum flux for a linear, steady-state, inviscid flow with diabatic forcing can be one of main differences between thermally induced waves and mechanically induced mountain waves. Because gravity wave drag on the large-scale flow is effective only where a vertical convergence/divergence of the momentum flux exists, gravity wave drag by thermal forcing can be more efficient than that by mountain even with the same amount of the momentum flux. In fact, the essence of parameterization schemes of orographically induced gravity wave drag in large-scale models has been to find the level of wave breaking where a vertical convergence/divergence of the momentum flux exists based on the theory by Eliassen and Palm (1960) for a linear, two-dimensional, steady-state, hydrostatic airflow over mountain.

In this paper, the momentum flux by thermally induced internal gravity waves and its approximation for use in large-scale models are investigated. For this, linear, two-dimensional, steady-state perturbations induced by diabatic heating, representing latent heating due to cumulus convection, in a uniform basic-state flow are considered. In section 2, simple but useful analytical formulations of the gravity wave momentum flux induced by thermal forcing and its vertical derivative are given. In section 3, approximation of the momentum flux as a gravity wave drag in large-scale models is presented. Some practical problems in using the proposed parameterization scheme in large-scale models are discussed in section 4. Summary and conclusions are given in the last section.

2. Theoretical basis

a. Governing equations and solutions

Consider a two-dimensional, steady-state, nonrotating, hydrostatic, inviscid, Boussinesq airflow system.

The equations governing small amplitude perturbations in a uniform basic-state horizontal wind with thermal forcing can be written as

$$U\frac{\partial u}{\partial x} + \frac{\partial \phi}{\partial x} = 0, \tag{1}$$

$$\frac{\partial \phi}{\partial z} = b, \tag{2}$$

$$U\frac{\partial b}{\partial x} + N^2 w = \frac{gQ}{c_p T_0}, \tag{3}$$

$$\frac{\partial u}{\partial x} + \frac{\partial w}{\partial z} = 0. \tag{4}$$

Here, u is the perturbation velocity in the x-direction, w the perturbation velocity in the z-direction, ϕ the perturbation kinematic pressure ($=p/\rho_0$, where p is the perturbation pressure and ρ_0 the basic-state density), b the perturbation buoyancy ($=g\theta/\theta_0$, where g is the gravitational acceleration, θ the perturbation potential temperature, and θ_0 the reference potential temperature), U the basic-state wind in the x-direction, N the buoyancy frequency, c_p the specific heat of air at constant pressure, T_0 the basic-state temperature, and Q the diabatic forcing. In this section, U and N are assumed to be horizontally uniform and constant with height. The basic-state wind considered in the following derivations is westerly, but the easterly basic-state wind case will be discussed in the momentum flux calculation. Equations (1)–(4) are the horizontal momentum equation in the x-direction, the hydrostatic equation, the thermodynamic energy equation, and the mass continuity equation, respectively.

Equations (1)–(4) can be combined into a single equation for the perturbation vertical velocity which, after taking the Fourier transform in x ($\rightarrow k$) (see the appendix for the definition of a one-sided Fourier transform pair), becomes

$$\frac{\partial^2 \hat{w}}{\partial z^2} + \frac{N^2}{U^2}\hat{w} = \frac{g\hat{Q}}{c_p T_0 U^2}. \tag{5}$$

The diabatic forcing Q is specified as

$$Q(x, z) = \begin{cases} 0 \\ \quad \text{for } 0 \le z < z_b, \\ Q_0\left(\dfrac{a_1^2}{x^2 + a_1^2} - \dfrac{a_1 a_2}{x^2 + a_2^2}\right) \\ \quad \text{for } z_b \le z \le z_t, \\ 0 \\ \quad \text{for } z > z_t, \end{cases} \tag{6}$$

where Q_0 is the magnitude of the diabatic forcing, a_1 is the half-width of the forcing function, and z_b and z_t denote the bottom and top heights of the forcing, respectively. The second term with a_2 ($>a_1$) in (6) is necessary to avoid a net forcing problem in a steady-state, nonrotating, inviscid flow (Smith and Lin 1982). Details for obtaining the perturbation vertical and horizontal velocities are given in the appendix.

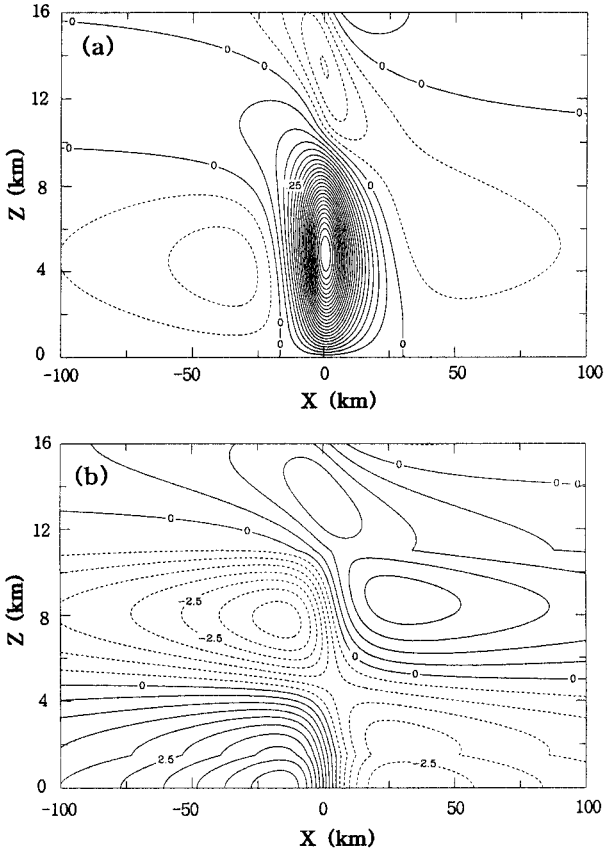

FIG. 1. The fields of (a) the perturbation vertical velocity by (A3) and (b) the perturbation horizontal velocity by (A5). The parameters used are $U = 15$ m s^{-1}, $N = 0.007$ s^{-1}, $z_b = 1.5$ km, $z_t = 11$ km, $a_1 = 10$ km, $a_2 = 5\ a_1$, $T_0 = 273$ K, and $Q_0 = 1$ J kg^{-1} s^{-1}. The contour intervals in (a) and (b) are 0.05 m s^{-1} and 0.5 m s^{-1}, respectively.

Figure 1 shows the perturbation vertical and horizontal velocity fields. The parameters specified are $U = 15$ m s^{-1}, $N = 0.007$ s^{-1}, $z_b = 1.5$ km, $z_t = 11$ km, $a_1 = 10$ km, $a_2 = 5\ a_1$, $T_0 = 273$ K, and $Q_0 = 1$ J kg^{-1} s^{-1}. There exist a strong updraft at the center of the specified heating region and relatively weak downdrafts on both upstream and downstream sides of the heating. The updraft in the upper part of the heating is slightly tilted upstream. Above the heating region, vertically propagating gravity waves with an upstream phase tilt are observed. The perturbation horizontal velocity field shows convergence in the lower troposphere and divergence above, which are responsible for the strong updraft in Fig. 1a. Because of the upstream tilt of waves, the perturbation horizontal velocity is stronger on the upstream side of the forcing than that on the downstream side.

b. Momentum flux

The vertical flux of integrated horizontal momentum M is defined by

$$M = \rho_0 \int_{-\infty}^{\infty} uw\, dx. \tag{7}$$

From the perturbation horizontal and vertical velocities given by (A5) and (A3) in the appendix, the momentum flux is shown to be expressed by

$$M = 0 \qquad \text{for } 0 \le z < z_b, \tag{8a}$$

$$M = -\rho_0 \pi a_1^2 \lambda \left(\frac{gQ_0}{c_p T_0 N^2}\right)^2 (\cos\lambda z_t - \cos\lambda z_b)(\cos\lambda z - \cos\lambda z_b) \ln\left[\frac{(a_1 + a_2)^2}{4a_1 a_2}\right] \qquad \text{for } z_b \le z \le z_t, \tag{8b}$$

$$M = -\rho_0 \pi a_1^2 \lambda \left(\frac{gQ_0}{c_p T_0 N^2}\right)^2 (\cos\lambda z_t - \cos\lambda z_b)^2 \ln\left[\frac{(a_1 + a_2)^2}{4a_1 a_2}\right] \qquad \text{for } z > z_t. \tag{8c}$$

The momentum flux below the diabatic forcing bottom is zero because downward propagating gravity waves from the forcing and reflected upward propagating gravity waves from the flat bottom completely cancel their momentum flux. The momentum flux in the forcing region varies with height and remains constant above it with the magnitude at the forcing top. As mentioned in the introduction, a vertical variation of the momentum flux in the diabatic forcing region for a linear, steady-state, inviscid system is one of the main differences between thermally induced waves and mechanically induced mountain waves. From (1) to (4), a relationship between the vertical wave energy flux and the momentum flux can be derived as

$$\int_{-\infty}^{\infty} \phi w\, dx = -U \int_{-\infty}^{\infty} uw\, dx. \tag{9}$$

Because the vertical wave energy flux is positive in order for waves to propagate upward, the momentum flux should be negative for the westerly ($U > 0$) basic-state wind and positive for the easterly ($U < 0$). The momentum flux given by (8) changes only its sign with the same magnitude if the easterly basic-state wind is considered instead of the westerly. As long as we consider the linear, steady-state, nonrotating, hydrostatic, inviscid, Boussinesq flow, a sign of the momentum flux is determined by a sign of the basic-state wind regardless of external forcing type such as mountain, diabatic heating, or diabatic cooling.

In a numerical study of convectively generated gravity waves by Fovell et al. (1992), the calculated wave momentum fluxes are all negative regardless of the direction of the stratospheric mean flow relative to the convective system. This result is associated with a westward tilt of waves for the three different basic-state wind cases in their study. In some sense, their mean flows in the stratosphere relative to the convective system are all westerly in reality because there are several convective cells in the simulated squall lines moving slower than the leading updraft. As long as gravity waves are generated by individual convective cells, the westward tilt of waves induced by convective cells behind the leading updraft is dominant. This is clearly seen in their momentum flux profile. That is, the westward tilt of waves in the stratosphere after sufficient time (6 h) for the three different mean flows somewhat resembles the linear, steady-state response of a stably stratified flow to diabatic heating under a westerly mean flow.

From (8), the vertical derivative of the momentum flux can be obtained by

$$\frac{dM}{dz} = \begin{cases} 0 & \text{for } 0 \le z < z_b, \\ \rho_0 \pi a_1^2 \lambda^2 \left(\dfrac{gQ_0}{c_p T_0 N^2}\right)^2 (\cos\lambda z_t - \cos\lambda z_b) \sin\lambda z \ln\left[\dfrac{(a_1 + a_2)^2}{4a_1 a_2}\right] & \text{for } z_b \le z \le z_t, \\ 0 & \text{for } z > z_t. \end{cases} \tag{10}$$

In general, the vertical derivative of the momentum flux is not defined at $z = z_b$ and z_t because it is not continuous at these levels even though the momentum flux itself is continuous there. If there is a specific relationship between λ ($=N/|U|$) and z_b such as $\lambda z_b = n\pi$, $n = 1, 2, 3, \ldots$, dM/dz becomes zero at $z = z_b$. Also, dM/dz becomes zero at $z = z_t$ when $\lambda z_t = n\pi$, $n = 1, 2, 3, \ldots$. Equation (10) indicates that the magnitude and sign of the vertical derivative of the momentum flux depend on the forcing top and bottom heights as well as the vertical wavenumber of dominant gravity waves ($\lambda_z = 2\pi|U|/N = 2\pi/\lambda$) for a given forcing structure. The absolute value of dM/dz becomes maximal when $z/\lambda_z = (2n + 1)/4$, $n = 0, 1, 2, 3, \ldots$. The above argument is true only when $\cos\lambda z_t - \cos\lambda z_b \neq 0$. If $\cos\lambda z_t - \cos\lambda z_b = 0$ by $z_t = z_b + \lambda_z n$, $n = 1, 2, 3, \ldots$, the momentum flux and its vertical derivative become zero at all the vertical levels.

There is another way to get the vertical derivative of the momentum flux. It can be obtained directly from the wave energy equation. From (1) to (4), it is straightforward to show that

$$\frac{dM}{dz} = -\frac{\rho_0 g}{c_p T_0 N^2 U}\int_{-\infty}^{\infty} bQ\, dx. \tag{11}$$

Here, the perturbation buoyancy can be expressed in terms of the perturbation horizontal velocity by

$$b(x, z) = -U\frac{\partial u}{\partial z}. \tag{12}$$

Outside the diabatic forcing region, (11) is reduced to the Eliassen–Palm theorem (Eliassen and Palm 1960). Note that (11) is valid for the case that the basic-state wind and stability vary with height as well as the case that they are uniform with height. When we consider the effect of gravity wave momentum flux on the large-scale flow, calculation of the vertical derivative of the momentum flux using (11) might be more straightforward than that using the perturbation horizontal and vertical velocities. In fact, the reason for deriving the momentum flux (8) is to estimate the momentum flux at the top of diabatic forcing that is transported into the upper atmosphere. The magnitude of the momentum flux at the forcing top corresponds to the maximum momentum flux that can be broken in the upper atmosphere. In analogy to mountain waves, the momentum flux at the top of diabatic forcing acts like the surface drag of mountain waves.

Figure 2 shows the vertical profiles of the momentum flux and its vertical derivative calculated using the same parameters in Fig. 1. The minimum momentum flux is about -3×10^4 N m^{-1}. At the heating top, the momentum flux is about -0.6×10^4 N m^{-1}. If the momentum flux in Fig. 2 is averaged over ~100 km, which is an order of the horizontal grid size in GCMs, the minimum momentum flux is about -0.3 N m^{-2} and the value at the heating top is about -0.06 N m^{-2}. This

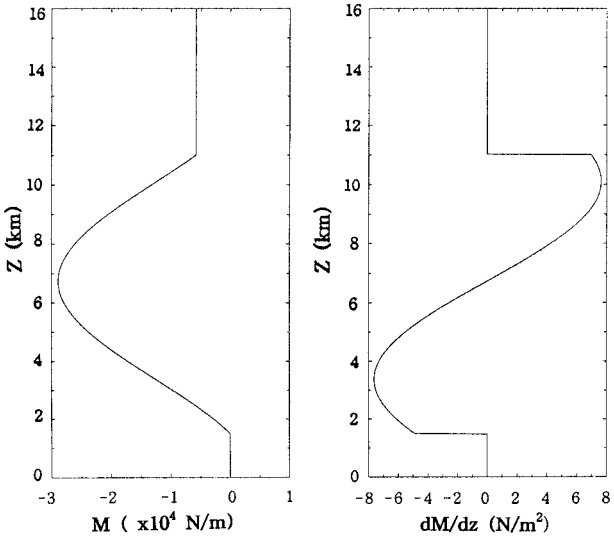

FIG. 2. The vertical profiles of the momentum flux by (8) (left panel) and its vertical derivative by (10) (right panel). The parameters used are the same as those in Fig. 1.

magnitude of the momentum flux at the heating top is small compared with that induced by numerically simulated squall lines by Fovell et al. (1992) (-0.2 N m^{-2}). Note that the parameter values used in Fig. 1 are chosen so as to be valid for a linear assumption. If this amount of the momentum flux is absorbed through breaking waves at 10 km above the heating top (21 km), the resultant zonal wind tendency by the wave momentum flux is about -6 m s^{-1} d^{-1} if the density at $z = 21$ km is assumed to be $\rho \sim \rho_0 e^{-z/H}$, where H is the scale height. This value is comparable to that by mountain in Palmer et al. (1986).

The vertical derivative of the momentum flux in Fig. 2b is negative from z_b (1.5 km) to 6.7 km and positive from 6.7 km to z_t (11 km). This implies that the westerly basic-state wind increases in the lower to middle troposphere and decreases in the middle to upper troposphere ($\partial\overline{u}/\partial t \propto -dM/dz$). If the easterly basic-state wind is considered, the vertical derivative of the momentum flux reverses its sign and the easterly basic-state wind also increases in the lower to middle troposphere and decreases in the middle to upper troposphere. Indeed, the sign and magnitude of the vertical derivative of the momentum flux are changed by the diabatic forcing structure and basic-state wind and stability. In the region of the diabatic heating, a maximum positive tendency of the zonal wind by the gravity wave momentum flux is about 10 m s^{-1} d^{-1} at $z = 3.4$ km, while a maximum negative tendency is about -24 m s^{-1} d^{-1} at $z = 10$ km for an exponentially decaying density profile. This is quite large compared with mountain-induced gravity wave drag.

There might be a question about the existence of gravity waves in the region of diabatic forcing representing cumulus convection that forms in a conditionally un-

stable environment. Even though it has been recognized that cumulus convection can generate gravity waves (Lin and Goff 1988) and gravity waves can trigger or enhance new or existing convective storms (Erickson and Whitney 1973; Uccellini 1975; Stobie et al. 1983), the general dynamic and thermodynamic structures of convective storms has not been considered as gravity waves. Recently, Pandya and Durran (1996) investigated mesoscale circulation around squall lines forced by steady thermal forcing using a two-dimensional numerical model. The dry simulation with steady thermal forcing reproduces most of the dynamic and thermodynamic structures of the convective storm including interior of the convective storm. The buoyancy frequency in the simulated squall lines is basically positive in most regions of the system except for in the well-mixed boundary layer and the low-level core of main updraft. They concluded that the circulation around squall lines can be regarded as gravity waves induced by steady thermal forcing.

c. Effect of basic-state wind on the momentum flux

The above formulations of the momentum flux and its vertical derivative are based on the westerly basic-state wind. As shown in (9), a sign of the gravity wave momentum flux is dependent upon the basic-state wind. If a convective system moves eastward with a constant speed (c) in a westerly basic-state wind, the basic-state wind relative to the moving system ($U - c$) can be negative. Also, in the tropical region where persistent convection exists, the basic-state wind itself can be negative. For an easterly basic-state case with the same governing equation set, it can be shown that the momentum flux and its vertical derivative are exactly the same as in (8) and (10) except for a sign change. This is indeed what we expect from the wave energy–momentum flux relationship.

A sign difference in the momentum flux is caused by the local momentum flux uw that is shown in Fig. 3 for the westerly and easterly basic-state wind cases. For the westerly (easterly) basic-state wind case, the upstream tilt of the negative (positive) momentum flux is dominant. However, for both the westerly and easterly basic-state wind cases, the momentum flux acts to accelerate the mean flow in the lower to middle troposphere and decelerate it in the middle to upper troposphere [i.e., westerly (easterly) increases in the lower to middle troposphere and decreases in the middle to upper troposphere]. Thus, this can result in an increase of vertical wind shear for both the cases, even though the uniform mean flow is considered in this study. This is also shown in Wu and Moncrieff (1996) who examined collective effects of organized convection, especially in the focus of the momentum flux, using a two-dimensional cloud model. The magnitude and shape of the momentum flux and its vertical derivative are comparable to those in this study except that the basic-state wind relative to the moving system is negative in their study. The only positive momentum flux in their study is located above the convective region, which is apparently induced by gravity waves. They showed that the negative momentum flux in the convective region is produced primarily by the front to rear ascent. This might be to some extent related to the nonlinear dynamics of convective system that is not considered in the present study.

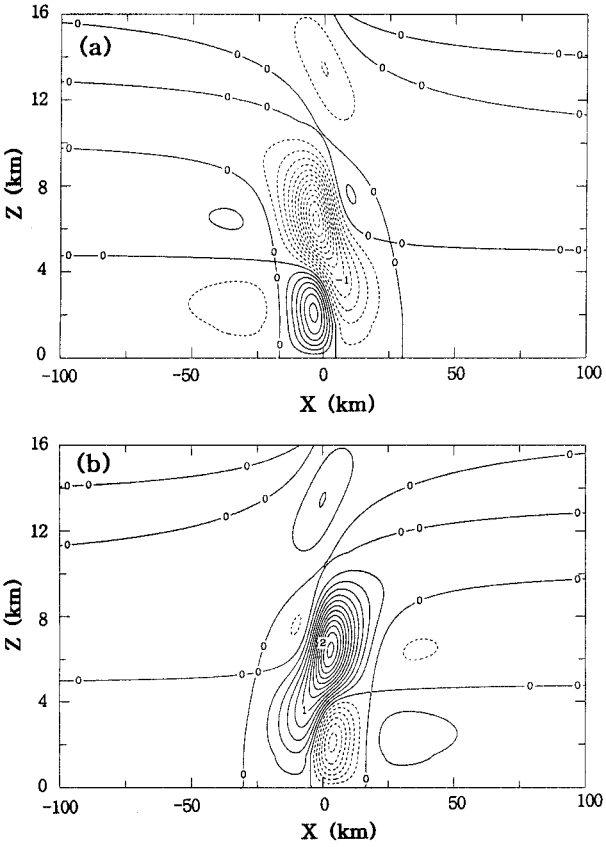

FIG. 3. The fields of the local momentum flux uw for the (a) westerly and (b) easterly basic-state wind cases. The parameters used are the same as those in Fig. 1. The contour interval is 0.2 m^2 s^{-2}.

The evaporative cooling of falling precipitation in the subcloud layer is not considered in this study. Although the cooling as diabatic forcing cannot change a sign of the momentum flux by the wave energy–momentum flux relationship, a resultant stability change in the cooling region makes a difference as shown in a numerical study by Pandya and Durran (1996). This is because the basic-state wind and stability are factors that influence the momentum flux in our system. The effects of stability on the response of a stably stratified uniform flow to thermal forcing were investigated by Chun (1995). She showed that wave reflectivity at the layer interface by a stability difference is less than one except for the case that the upper layer is neutrally stratified. For a neutrally stratified upper atmosphere, there is no steady-state solution because resonance can happen in the lower layer. Without over-

reflection, the momentum flux cannot change its sign. The only possibility of the negative momentum flux for the easterly basic-state wind (or system relative mean flow) is in the case that a critical level is located in a dynamically unstable mean flow (Chun and Lin 1995). Because a main focus of this section lies in the analytical formulations of the momentum flux induced by diabatic forcing and its vertical derivative, the effects of stability and critical-level reflection are not included for simplicity. This problem, difficult to handle analytically, remains to be investigated.

3. Parameterization of convection-induced momentum flux in large-scale models

The effects of subgrid-scale momentum flux induced by convection on the grid-scale flow can be quantitatively represented in large-scale models through parameterization. As in the parameterization of orographically induced gravity wave drag in GCMs, it is not straightforward to implement this process into large-scale models because the momentum flux and its vertical derivative are derived based on a simplified flow system compared with the real atmosphere.

The role of the gravity wave momentum flux in the large-scale flow as a drag owing to subgrid-scale eddies can be included in the horizontal momentum equation by

$$\frac{\partial \overline{u}}{\partial t} = -\frac{1}{\rho}\frac{\partial \tau_x}{\partial z}, \tag{13}$$

where $\overline{u}$ is the grid-resolvable zonal wind and τ_x the subgrid-scale zonal momentum flux defined by

$$\tau_x = \int \rho u' w' \, dx/\Delta x. \tag{14}$$

Here, u' and w' are the unresolvable subgrid-scale zonal and vertical velocities, respectively, and Δx is the grid size in the zonal direction. The integral in (14) is taken over the grid interval. From the definition of the momentum flux given by (7), the zonal momentum flux can be approximated by

$$\tau_x \simeq M/\Delta x. \tag{15}$$

A vertical profile of τ_x can be obtained using the analytical formulation of the momentum flux (8) from the surface to above the cloud top, in principle.

Parameterizing subgrid-scale convection-induced gravity wave momentum flux for use in large-scale models inherently requires some information from subgrid-scale cumulus parameterization. Cumulus parameterization schemes currently used in GCMs can be categorized into the mass-flux scheme, the moisture convergence scheme, and the convective adjustment scheme. These cumulus parameterization schemes are activated only when the model atmosphere at each grid-point is found to be conditionally unstable. Thus, it appears to be difficult to take account of internal gravity waves in a conditionally unstable atmosphere, where cumulus convection exists, in a present viewpoint of large-scale modeling. However, in the atmosphere above the cloud-top height, convection-induced gravity waves can propagate and affect the large-scale flow. For this reason, it is suggested that in large-scale models convection-induced gravity wave momentum flux be considered in the region above the cloud-top height but not considered inside the cloud region. The momentum flux from the surface to cloud-base height is not considered because it is zero according to the simple calculation (8a). Thus, the following parameterization scheme for convection-induced gravity wave momentum flux in large-scale models is designed to be activated from cloud-top height.

The analytical expression of the momentum flux M for $z \geq z_t$ can be rewritten as

$$M = -(\rho_0 U^3/N)c_1 c_2^2 \mu^2. \tag{16}$$

The parameter c_1, defined by $\pi \ln[(a_1 + a_2)^2/4a_1a_2]$, is related to the horizontal structure of thermal forcing. The parameter c_2, defined by $\cos\lambda z_t - \cos\lambda z_b$, is related to the basic-state wind and stability and the bottom and top heights of thermal forcing. The parameter μ is the nonlinearity factor of thermally induced internal gravity waves (Lin and Chun 1991; Chun and Baik 1994) defined by

$$\mu = \frac{gQ_0 a_1}{c_p T_0 N U^2}. \tag{17}$$

Note that in numerical models the basic-state wind U in (16) and (17) is the zonal wind $\overline{u}$.

Using (15) and (16), the zonal momentum flux is given by

$$\tau_x = -[\rho U^3/(N\Delta x)]G(\mu), \tag{18}$$

where

$$G(\mu) = c_1 c_2^2 \mu^2. \tag{19}$$

In (18), the constant basic-state density ρ_0 in (16), which comes from the Boussinesq approximation, is replaced by the local density ρ. There is an analogy between the formulation of τ_x given by (18) and that of orographically induced wave drag given by Pierrehumbert (1986) except that in his case the Froude number instead of μ appears. This is somewhat expected because the inverse Froude number (Nh/U, where h is the mountain height) is the nonlinearity factor of mountain waves. Note that the momentum flux M in (8) and (16) is derived under a linear assumption. For an upper bound of large μ, a form of $G(\mu)$ given by

$$G(\mu) = \frac{c_1 c_2^2 \mu^2}{1 + \mu^2} \tag{20}$$

may be used just following a functional form by Pierrehumbert (1986), even though a systematic numerical study of thermally induced momentum flux with varying nonlinearity factors has not been done yet to support (20) or provide another form.

There are two basic steps considered in this study to parameterize the momentum flux induced by thermal forcing. The first step is to find the analytical expression of the momentum flux at the top of thermal forcing, as is done in (18). The second step is to find the momentum flux redistributed above the forcing top in terms of the nonlinearity factor μ. For mountain drag parameterization, there are currently two types of schemes to handle the second step. The schemes are grouped according to whether the scheme employs the Lindzen's (1981) saturation hypothesis in terms of the Richardson number criterion or assumes a linear decrease of reference level flux to zero at the model top (Kim 1996).

For use of the saturation hypothesis, the Richardson number criterion for thermally induced waves should be obtained. From (A3) and (A5), the total stability squared and vertical shear including the basic-state flow and wave impact above the forcing top can be expressed, respectively, by

$$N_T^2 = N^2[1 + c_2\mu(X_3' \sin\lambda z + X_4' \cos\lambda z)], \quad (21)$$

$$\eta_T = \eta[1 + c_2\mu \mathrm{Ri}^{1/2}(X_3' \cos\lambda z - X_4' \sin\lambda z)], \quad (22)$$

where η is the vertical shear (dU/dz), Ri is the Richardson number defined by N^2/η^2, $X_3' = X_3/a_1$, and $X_4' = X_4/a_1$. These expressions of N_T^2 and η_T are basically similar to those in Palmer et al. (1986) except for the terms inside parentheses. This is because we consider an infinite number of waves induced by isolated thermal forcing, while they considered a monochromatic wave over a sinusoidal mountain. From (21) and (22), it may be approximated that

$$\mathrm{Ri}_{\min} \simeq \frac{\mathrm{Ri}(1 - \mu|c_2|)}{(1 + \mu \mathrm{Ri}^{1/2}|c_2|)^2}, \quad (23)$$

where $\mathrm{Ri}_{\min}$ is the minimum Richardson number that can hold under the influence of waves. Note that c_2 can be either positive or negative depending on the structure of the basic-state wind and stability and the cloud bottom and top heights. When $\mathrm{Ri}_{\min}$ is set to ¼ based on Lindzen's (1981) saturation hypothesis, the nonlinearity factor for wave saturation can be derived by

$$\mu_s = \frac{1}{|c_2|}\left[2\sqrt{2 + \frac{1}{\sqrt{\mathrm{Ri}}}} - \left(2 + \frac{1}{\sqrt{\mathrm{Ri}}}\right)\right]. \quad (24)$$

For the parameters used in Fig. 1 ($|c_2| \sim 0.36$), μ_s is about 2 for Ri = 10 and approaches 2.3 for Ri $\to \infty$.

Then, from (18) and (19), the saturation zonal momentum flux is given by

$$\tau_s = -[\rho U^3/(N\Delta x)]c_1 c_2^2 \mu_s^2. \quad (25)$$

This formulation indicates a strong dependency of τ_s on U as in the mountain wave case by Palmer et al. (1986). Thus, wave breaking might be possible in the region of weak basic-state wind. If we consider a situation in the lower stratosphere with $N = 0.02$ s^{-1}, $\rho = 0.05$ kg m^{-3}, and $\Delta x = 100$ km, the momentum flux at the cloud top numerically calculated by Fovell et al. (1992) (-0.2 N m^{-2}) might be broken when U is less than 18.5 m s^{-1} for $\mu_s = 2.3$ with the parameter values of c_1 and c_2 used in Fig. 1. This value of U is close to that in Palmer et al. (1986) (15 m s^{-1}), which is not climatologically unreasonable. Thus, the lower stratosphere with $U < 18.5$ m s^{-1} might be a preferable region of wave breaking with the above parameter set.

The methodology for parameterizing the zonal momentum flux induced by thermal forcing proposed in this study can be summarized as follows. From the cloud-base to cloud-top height, the effect of the momentum flux induced by subgrid-scale diabatic forcing is not considered because subgrid-scale cumulus convection in large-scale models is only activated in a conditionally unstable atmosphere. Below the cloud base, the momentum flux is also not considered because of the wave momentum cancellation. At the cloud top, the momentum flux is obtained by (18) and (19). If the nonlinearity factor is large enough, (20) or another form instead of (19) can be used. Above the cloud top, there are two ways to construct the momentum flux profile. One way is to specify a vertical structure of the momentum flux normalized by the cloud-top value, similar to what has been done for mountain drag parameterization (e.g., Iwasaki et al. 1989; Broccoli and Manabe 1992). The other way is to apply the wave saturation hypothesis in order to find wave breaking levels in terms of the Richardson number criterion using the nonlinearity factor of thermally induced waves. That is, if $\mathrm{Ri}_{\min} \geq$ ¼, the momentum flux at a certain level above the cloud top is equal to that below that level, while if $\mathrm{Ri}_{\min} <$ ¼, the saturation momentum flux given by (25) is used. This procedure is repeated until the model top is reached. At the model top, the momentum flux can be specified as either zero or a value just below it. The method employing the wave saturation hypothesis is essentially the same as that which has been used in mountain wave drag parameterization (Kim 1996).

4. Some practical problems in large-scale models and discussion

There are several practical problems when the above proposed scheme is used in large-scale models. First, the magnitude of diabatic forcing Q_0 and the half-width of diabatic forcing a_1 are needed to compute the nonlinearity factor of thermally induced gravity waves μ [see (17)]. A product of these two parameters is approximated as follows. The grid-averaged subgrid-scale diabatic heating due to cumulus convection, which is evaluated using a cumulus parameterization scheme, is represented by $\overline{Q} = \alpha Q_1 + (1 - \alpha)Q_2 \cong \alpha Q_1$, where α is the fractional coverage of subgrid-scale cumulus clouds in a grid box, Q_1 the cumulus heating that is equivalent to Q_0, and Q_2 the thermal forcing outside the cumulus cloud region. The parameter a_1, which represents half of the horizontal scale of diabatic forcing, might be approximated by $\alpha\Delta x/2$. Therefore, $Q_0 a_1$ can

be approximated by $\overline{Q}\Delta x/2$. Although the fractional coverage of subgrid-scale cumulus clouds is mentioned here, we do not actually need it for computing the nonlinearity factor. In this way, there appears a dependency of the nonlinearity factor on the horizontal grid size. However, it is noted that in large-scale models as the horizontal grid size increases (decreases), the subgrid-scale diabatic heating due to cumulus convection tends to become small (large).

Second, the magnitude of diabatic forcing Q_0 and the basic-state wind U and stability N are assumed to be constant with height in order to simplify the problem and obtain the analytical formulation of the momentum flux. This assumption is not strictly valid in reality. However, for the parameterization of subgrid-scale momentum flux in large-scale models, Q_0, U, and N can be taken to be averaged, to a first approximation, from the cloud base to cloud top. Determining the cloud base and top heights and computing the subgrid-scale diabatic heating are accomplished with cumulus parameterization.

Third, the minimum Richardson number, saturation nonlinearity factor, and momentum flux are sensitive to the parameter c_2 ($=\cos\lambda z_t - \cos\lambda z_b$). This parameter value lies between -2 and 2. The momentum flux is zero at all the vertical levels if $c_2 = 0$. If the absolute magnitude of c_2 is close to zero, $\mathrm{Ri}_{\min}$ approaches Ri and μ_s becomes very large [see (23) and (24)]. That is, it is difficult for gravity waves to break. The magnitude of c_2 itself is sensitive to the basic-state wind and stability and the cloud-base and -top heights. Even though c_2 can have any value for a given parameter set, it might be bounded based on a critical value of the nonlinearity factor of thermally induced waves. Baik and Chun (1996) found a critical value of the nonlinearity factor for wave overturning ($\mu_s \sim 2.2$) in the uniform basic-state wind case ($\mathrm{Ri} \to \infty$), which might give a bounded value of $|c_2| \sim 0.38$. However, because the critical value is obtained with a fixed value of nondimensional heating depth (or inverse of the thermal Froude number), a further systematic numerical study is needed to find critical value of the nonlinearity factor for wave overturning with various thermal Froude numbers. The parameter c_1, which is related to the horizontal structure of thermal forcing, is a constant determined by a ratio of a_1 to a_2. Because a_2 represents a widespread minor forcing that has an opposite sign to the localized main forcing with a half-width of a_1, it is somewhat arbitrary. It might be recommended to use $a_2 = 5a_1$ as used in several analytical studies (Smith and Lin 1982; Baik 1992; Chun and Baik 1994). However, some sensitivity experiments in large-scale models are required to get a suitable ratio of a_1 to a_2.

Fourth, there is a dependency of the momentum flux and saturation momentum flux on the horizontal grid interval Δx in (18) and (25). For mountain drag parameterization, the number of mountains (m) is multiplied in the momentum flux formula and then $m/\Delta x$ is just specified as a tuning coefficient. In our case, the proposed parameterization scheme is influenced by Δx.

Fifth, the above discussion is based on the two-dimensional assumption with unidirectional wind and x-dependent thermal forcing. It is not easy to derive an analytical form of the momentum flux for a three-dimensional flow system with generalized thermal forcing. However, in three-dimensional models the basic-state wind in the scheme might be regarded as the basic-state wind projected on a certain reference level (say, cloud-top height). Then, τ_x and τ_y can be obtained by decomposing the two-dimensional form of τ [equivalent to (18)] as was done in mountain drag parameterization (e.g., Palmer et al. 1986).

It seems that one of the main points needed to improve the proposed scheme is to relax the assumption on the basic-state wind. It has been well known from theoretical and numerical modeling studies (e.g., Thorpe et al. 1982; Weisman and Klemp 1982; Rotunno et al. 1988) that vertical shear of the basic-state wind is a crucial factor in maintaining convective systems. Even though the uniform basic-state wind is assumed in order to simplify the problem and derive the analytical form of the momentum flux, it may not be very realistic, especially for the atmospheric condition related to convective systems. For the uniform basic-state wind case, relative wind with respect to convection is theoretically zero if convection moves with the basic-state wind at some level. In this case, no flow passes the wave generator. However, when the proposed scheme with constant basic-state wind is applied in large-scale models, the effects of wind shear will be included by using local wind at each grid point as done in Palmer et al. (1986). In the analytical formulation of the momentum flux by convection, Kershaw (1995) even deduced a linear relationship between the wind shear and the momentum flux under the assumption of constant basic-state wind. Including vertical wind shear in the proposed scheme remains to be investigated.

5. Summary and conclusions

The dynamical role of gravity wave momentum flux in the large-scale mean flow has been well recognized by many theoreticians and numerical modelers. Orographically induced gravity wave drag has a beneficial effect on simulated large-scale features. Even though the source of gravity waves considered thus far in the parameterization of subgrid-scale momentum flux in large-scale models has exclusively been the mountains, the effects of mountain drag can be relatively weak in certain atmospheric conditions such as during summertime with weak surface wind and stability and in the tropical region where persistent cumulus convection exists. Under these situations, cumulus convection can be an alternative source of gravity waves influencing the large-scale mean flow as a subgrid-scale drag.

In this study, we analytically investigated the mo-

mentum flux induced by thermal forcing, representing latent heating due to cumulus convection, and proposed a way to parameterize the momentum flux in large-scale models. For this, we revisited linear, two-dimensional, steady-state, nonrotating, hydrostatic, inviscid perturbations induced by specified thermal forcing in a Boussinesq flow under a uniform basic-state wind. From this simplified flow system, we derived analytical forms of the vertical flux of integrated horizontal momentum and its vertical derivative. The momentum flux below the forcing bottom is zero because downward propagating gravity waves from the forcing and reflected upgoing gravity waves from the flat bottom cancel their momentum flux completely. Inside the forcing region, the momentum flux varies with height up to the forcing top and remains constant above it. With a reasonable parameter set satisfying a linear assumption, the magnitude of the calculated momentum flux and its impact on the zonal mean flow tendency were shown to be even larger than those in mountain drag. A nonzero vertical convergence or divergence of the momentum flux in the thermal forcing region especially distinguishes this process from mountain drag. The maximum magnitude of the zonal mean flow tendency due to the momentum flux in the forcing region is as large as 24 m s^{-1} d^{-1}.

We outlined a possible way for parameterizing convection-induced subgrid-scale gravity wave momentum flux in large-scale models. For the momentum flux profile up to the cloud-top height, use of the linear analytical form was suggested. However, the effect of convection-induced gravity wave momentum flux in large-scale models is included only above the cloud-top height because subgrid-scale cumulus parameterization is activated in a conditionally unstable atmosphere. Thus, the proposed scheme is designed to activate in the region above cloud-top height. The formulation of the momentum flux at the cloud top that can be broken in the upper atmosphere was shown to be similar to that of the surface drag of mountain waves by using the nonlinearity factor of thermally induced waves that is analogous to the inverse Froude number in mountain waves. A vertical profile of redistributed momentum flux above the cloud top can be approximated either by specifying a functional form or by using the wave saturation hypothesis in terms of the Richardson number criterion. The formulation of the minimum Richardson number including wave impact is similar to that in the mountain wave case. Basically, the proposed scheme to parameterize the momentum flux above the cloud top is similar to mountain drag parameterization as long as the nonlinearity factor of thermally induced waves is used appropriately.

Several practical problems in the proposed scheme when it is used in large-scale models were discussed. The magnitude of diabatic forcing and the half-width of forcing are needed to compute the nonlinearity factor of thermally induced waves. It was shown that a product of these two parameters is somewhat influenced by the horizontal grid size. We discussed the assumption of the height-independent diabatic forcing magnitude and basic-state wind and stability. There are two constants (c_1 and c_2) in the formulation of the momentum flux. The parameter c_2 is sensitive to the basic-state wind and stability and the cloud-base and -top heights. The momentum flux is sensitive to the value of c_2. However, the magnitude of c_2 can be bounded based on a critical nonlinearity factor of thermally induced waves. We pointed out that the proposed scheme depends on the horizontal grid size. Finally, we discussed the two-dimensional limitation of the scheme and in three-dimensional models suggested following the method used in mountain drag parameterization.

In this study, we assumed a vertically uniform basic-state wind to simplify the problem. This assumption needs to be relaxed when applying the proposed scheme to baroclinic zones where vertical shear is important. Further study along this line is needed. In this study, we did not yet perform three-dimensional numerical model experiments with the proposed scheme. But, the effects of subgrid-scale convection-induced gravity wave momentum flux on simulated large-scale features are planned to be investigated using a GCM. In particular, the large-scale flow pattern in the tropical upper atmosphere related to internal gravity waves such as quasi-biennial oscillation is hoped to be better simulated by including the proposed parameterization of gravity wave drag by convection. In this study, we exclusively considered the momentum flux induced by gravity waves. When there exists mesoscale convective clouds, momentum flux by convection itself in the cloud region might be much larger than that by convectively gerenated gravity waves above the cloud region. This means that the change in the mean flow in the cloud region by cloud momentum flux should not be ignored, which is not resolved in large-scale models. However, it seems that a way to parameterize cloud momentum flux in a conditionally unstable atmosphere should be different from what was done in this study.

Acknowledgments. The first author was supported by the 1996 Yonsei University Research Fund. The second author was supported by the Korea Ministry of Science and Technology. The authors would like to thank the reviewers for providing valuable comments on this study.

APPENDIX

Analytical Solutions for the Perturbation Vertical and Horizontal Velocities

A one-sided Fourier transform pair is defined by

$$\hat{w}(k, z) = \frac{1}{\pi}\int_{-\infty}^{\infty} w(x, z)e^{-ikx}\,dx, \tag{A1a}$$

$$w(x, z) = \mathrm{Re}\left\{\int_{0}^{\infty} \hat{w}(k, z)e^{ikx}\,dk\right\}. \tag{A1b}$$

The general solution of (5) can be written as

$$\hat{w}(k, z) = Ae^{i\lambda z} + Be^{-i\lambda z} \quad \text{for } 0 \le z < z_b, \tag{A2a}$$

$$\hat{w}(k, z) = Ce^{i\lambda(z-z_b)} + De^{-i\lambda(z-z_b)} + \frac{g\hat{Q}}{c_pT_0N^2} \quad \text{for } z_b \le z \le z_t, \tag{A2b}$$

$$\hat{w}(k, z) = Ee^{i\lambda(z-z_t)} + Fe^{-i\lambda(z-z_t)} \quad \text{for } z > z_t, \tag{A2c}$$

where $\lambda = N/|U|$. The six unknown coefficients (A, B, C, D, E, and F) are arbitrary functions of k to be determined by boundary and interface conditions. The flat-bottom boundary condition of $\hat{w} = 0$ at $z = 0$ gives $A = -B$ and the upper radiation boundary condition allowing waves to propagate upward without any reflection requires $F = 0$ for $U > 0$ (Booker and Bretherton 1967). In addition, we have interface conditions that both $\hat{w}$ and $\partial\hat{w}/\partial z$ are continuous at $z = z_b$ and z_t. Taking the inverse Fourier transform after applying the boundary and interface conditions to (A2), we obtain

$$w(x, z) = \frac{gQ_0}{c_pT_0N^2}[-X_1(\sin\lambda z_t - \sin\lambda z_b) - X_2(\cos\lambda z_t - \cos\lambda z_b)]\sin\lambda z \quad \text{for } 0 \le z < z_b, \tag{A3a}$$

$$w(x, z) = \frac{gQ_0}{c_pT_0N^2}[X_1(-\cos\lambda z_b\cos\lambda z - \sin\lambda z_t\sin\lambda z + 1) - X_2(\cos\lambda z_t - \cos\lambda z_b)\sin\lambda z] \quad \text{for } z_b \le z \le z_t, \tag{A3b}$$

$$w(x, z) = \frac{gQ_0}{c_pT_0N^2}(\cos\lambda z_t - \cos\lambda z_b)[X_1\cos\lambda z - X_2\sin\lambda z] \quad \text{for } z > z_t, \tag{A3c}$$

where

$$X_1 = \frac{a_1^2}{x^2 + a_1^2} - \frac{a_1a_2}{x^2 + a_2^2},$$

$$X_2 = \frac{a_1x}{x^2 + a_1^2} - \frac{a_1x}{x^2 + a_2^2}.$$

From (4), the perturbation horizontal velocity can be obtained using

$$u(x, z) = -\int_{-\infty}^{x} \frac{\partial w}{\partial z}\, dx, \tag{A4}$$

which gives

$$u(x, z) = \frac{gQ_0}{c_pT_0N^2}\lambda[X_3(\sin\lambda z_t - \sin\lambda z_b) + X_4(\cos\lambda z_t - \cos\lambda z_b)]\cos\lambda z \quad \text{for } 0 \le z < z_b, \tag{A5a}$$

$$u(x, z) = \frac{gQ_0}{c_pT_0N^2}\lambda[-X_3(\cos\lambda z_b\sin\lambda z - \sin\lambda z_t\cos\lambda z) + X_4(\cos\lambda z_t - \cos\lambda z_b)\cos\lambda z] \quad \text{for } z_b \le z \le z_t, \tag{A5b}$$

$$u(x, z) = \frac{gQ_0}{c_pT_0N^2}\lambda(\cos\lambda z_t - \cos\lambda z_b)[X_3\sin\lambda z + X_4\cos\lambda z] \quad \text{for } z > z_t, \tag{A5c}$$

where

$$X_3 = a_1\left(\tan^{-1}\frac{x}{a_1} - \tan^{-1}\frac{x}{a_2}\right),$$

$$X_4 = \frac{a_1}{2}\ln\left(\frac{x^2 + a_1^2}{x^2 + a_2^2}\right).$$

REFERENCES

Baik, J.-J., 1992: Response of a stably stratified atmosphere to low-level heating—An application to the heat island problem. *J. Appl. Meteor.*, **31,** 291–303.

——, and H.-Y. Chun, 1996: Effects of nonlinearity on the atmospheric flow response to low-level heating in a uniform flow. *J. Atmos. Sci.*, **53,** 1856–1869.

Booker, J. R., and F. P. Bretherton, 1967: The critical layer for internal gravity waves in a shear flow. *J. Fluid Mech.*, **27,** 513–539.

Broccoli, A. J., and S. Manabe, 1992: The effects of orography on midlatitude northern hemisphere dry climates. *J. Climate*, **5,** 1181–1201.

Chun, H.-Y., 1995: Enhanced response of a stably stratified two-layer atmosphere to low-level heating. *J. Meteor. Soc. Japan,* **73,** 685–696.

——, 1997: Weakly nonlinear response of a stably stratified shear flow to thermal forcing. *Tellus,* **49A,** 528–543.

——, and J.-J. Baik, 1994: Weakly nonlinear response of a stably stratified atmosphere to diabatic forcing in a uniform flow. *J. Atmos. Sci.,* **51,** 3109–3121.

——, and Y.-L. Lin, 1995: Enhanced response of an atmospheric flow to a line-type heat sink in the presence of a critical level. *Meteor. Atmos. Phys.,* **55,** 33–45.

Clark, T. L., T. Hauf, and J. P. Kuettner, 1986: Convectively forced internal gravity waves: Results from two-dimensional numerical experiments. *Quart. J. Roy. Meteor. Soc.,* **112,** 899–925.

Eliassen, A., and E. Palm, 1960: On the transfer of energy in stationary mountain waves. *Geofys. Publ.,* **22,** 1–23.

Erickson, C. O., and L. F. Whitney Jr., 1973: Gravity waves following severe thunderstorms. *Mon. Wea. Rev.,* **101,** 708–711.

Fovell, R., D. Durran, and J. R. Holton, 1992: Numerical simulations of convectively generated stratospheric gravity waves. *J. Atmos. Sci.,* **49,** 1427–1442.

Fritts, D. C., 1984: Gravity wave saturation in the middle atmosphere: A review of theory and observations. *Rev. Geophys. Space Phys.,* **22,** 275–308.

Iwasaki, T., S. Yamada, and K. Tada, 1989: A parameterization scheme of orographic gravity wave drag with two different vertical partitionings. Part I: Impacts on medium-range forecasts. *J. Meteor. Soc. Japan,* **67,** 11–27.

Kershaw, R., 1995: Parameterization of momentum transport by convectively generated gravity waves. *Quart. J. Roy. Meteor. Soc.,* **121,** 1023–1040.

Kim, Y.-J., 1996: Representation of subgrid-scale orographic effects in a general cirulation model. Part I: Impact on the dynamics of simulated January climate. *J. Climate,* **9,** 2698–2717.

Lin, Y.-L., 1987: Two-dimensional response of a stably stratified shear flow to diabatic heating. *J. Atmos. Sci.,* **44,** 1375–1393.

——, and R. C. Goff, 1988: A study of a mesoscale solitary wave in the atmosphere originating near a region of deep convection. *J. Atmos. Sci.,* **45,** 194–205.

——, and H.-Y. Chun, 1991: Effects of diabatic cooling in a shear flow with a critical level. *J. Atmos. Sci.,* **48,** 2476–2491.

Lindzen, R. S., 1981: Turbulence and stress due to gravity wave and tidal breakdown. *J. Geophys. Res.,* **86,** 9707–9714.

McFarlane, N. A., 1987: The effect of orographically excited gravity wave drag on the general circulation of the lower stratosphere and troposphere. *J. Atmos. Sci.,* **44,** 1775–1800.

Palmer, T. N., G. J. Shutts, and R. Swinbank, 1986: Alleviation of a systematic westerly bias in circulation and numerical weather prediction model through an orographic gravity wave drag parameterization. *Quart. J. Roy. Meteor. Soc.,* **112,** 1001–1039.

Pandya, R. E., and D. Durran, 1996: The influence of convectively generated thermal forcing in the mesoscale circulation around squall lines. *J. Atmos. Sci.,* **53,** 2924–2951.

Pierrehumbert, R. T., 1986: An essay on the parameterization of orographic gravity wave drag. *Proc. Seminar/Workshop on Observation, Theory, and Modeling of Orographic Effects,* Vol. 1, Reading, United Kingdom, ECMWF, 251–282.

Rotunno, R., J. B. Klemp, and M. L. Weisman, 1988: A theory for strong, long-lived squall lines. *J. Atmos. Sci.,* **45,** 463–485.

Smith, R. B., and Y.-L. Lin, 1982: The addition of heat to a stratified airstream with application to the dynamics of orographic rain. *Quart. J. Roy. Meteor. Soc.,* **108,** 353–378.

Stobie, J. G., F. Einaudi, and L. W. Uccellini, 1983; A case study of gravity waves-convective storms interaction: 9 May 1979. *J. Atmos. Sci.,* **40,** 2804–2830.

Swinbank, R., 1985: The global atmospheric angular momentum balance inferred from analyses made during the FGGE. *Quart. J. Roy. Meteor. Soc.,* **111,** 977–992.

Thorpe, A. J., M. J. Miller, and M. W. Moncrieff, 1982: Two-dimensional convection in non-constant shear: A model of mid-latitude squall lines. *Quart. J. Roy. Meteor. Soc.,* **108,** 739–762.

Uccellini, L. W., 1975: A case study of apparent gravity-wave initiation of severe convective storms. *Mon. Wea. Rev.,* **103,** 497–513.

Weisman, M. L., and J. B. Klemp, 1982: The dependence of numerically simulated convective storms on vertical wind shear and buoyancy. *Mon. Wea. Rev.,* **110,** 504–520.

Wu, X., and M. Moncrieff, 1996: Collective effects of organized convection and their approximation in general circulation models. *J. Atmos. Sci.,* **53,** 1477–1495.